

Non-Orthogonal Multiple Access System for 5G Networks



By

Soma Qureshi

NUST201464080MSEEC61214F

Supervisor

Dr. Syed Ali Hassan

Department of Electrical Engineering

A thesis submitted in partial fulfillment of the requirements for the degree
of Masters of Science in Electrical Engineering (MS EE)

In

School of Electrical Engineering and Computer Science,
National University of Sciences and Technology (NUST),

Islamabad, Pakistan.

(December 29, 2016)

Approval

It is certified that the contents and form of the thesis entitled “**Non-Orthogonal Multiple Access System for 5G Networks**” submitted by Soma Qureshi have been found satisfactory for the requirement of the degree.

Advisor: **Dr. Syed Ali Hassan**

Signature: _____

Date: _____

Committee Member 1: **Dr. Sajid Saleem**

Signature: _____

Date: _____

Committee Member 2: **Dr. Fahd Ahmed Khan**

Signature: _____

Date: _____

Committee Member 3: **Dr. Rizwan Ahmad**

Signature: _____

Date: _____

Abstract

From the past few years, the demand for higher data rates has become increasingly important. Non-orthogonal multiple access (NOMA) has emerged as a candidate multiple access technique to meet this overwhelming demand of data traffic in fifth generation (5G) of wireless networks. In this thesis, we investigate a new spectrum sharing strategy using NOMA. The proposed scheme, successive bandwidth division (SBD)-NOMA, is a hybrid approach exploiting characteristics of both the conventional NOMA system and the orthogonal multiple access (OMA) system. The performance of the proposed scheme is evaluated with a constant power allocation coefficients using a criteria of sum capacity, outage capacity and energy efficiency. Power allocation is being performed in SBD-NOMA to maximize the sum rate using a divide-and-allocate approach such that all users are allocated with an optimal transmission power. The performance comparison of this scheme is made with conventional NOMA scheme and other existing power allocation schemes. Under Rayleigh fading, the probability density function (PDF) of the received signal-to-interference plus noise ratio (SINR) is derived and closed-form expressions for the outage probability are presented when channel state information (CSI) is available at the base station (BS). The performance is evaluated in terms of receiver complexity, average sum rate and outage probability. Simulations results are provided to access and

compare the performance of the proposed scheme with other contemporary approaches.

Dedication

I dedicate this thesis to my Parents and Faculty.

Certificate of Originality

I hereby declare that this submission is my own work and to the best of my knowledge it contains no materials previously published or written by another person, nor material which to a substantial extent has been accepted for the award of any degree or diploma at NUST SEECS or at any other educational institute, except where due acknowledgement has been made in the thesis. Any contribution made to the research by others, with whom I have worked at NUST SEECS or elsewhere, is explicitly acknowledged in the thesis.

I also declare that the intellectual content of this thesis is the product of my own work, except for the assistance from others in the project's design and conception or in style, presentation and linguistics which has been acknowledged.

Author Name: Soma Qureshi

Signature: _____

Acknowledgment

I would like to thank my project supervisor Dr. Syed Ali Hassan for his cooperation and support to bring this dissertation to completion. I would also like to thank my family and friends for their continuous encouragement and moral support.

Table of Contents

1	Introduction	xii
1.1	Introduction to 5G	xii
1.2	Multiple Access Schemes	xiii
1.2.1	Orthogonal multiple access	xiii
1.2.2	Non-Orthogonal multiple access	xiv
1.3	Motivation	xv
1.4	Problem Statement	xviii
1.5	Thesis Contribution	xviii
1.6	Thesis Organization	xix
2	Background and Literature Review	xx
2.1	NOMA	xx
3	Successive Bandwidth Division NOMA system	xxii
3.1	System Model	xxiii
3.1.1	Proposed SBD Scheme	xxiv
3.1.2	Received Signal Model for proposed UL SBD-NOMA	xxvi
3.1.3	Received SINR	xxviii
3.2	Proposed Channel Allocation Algorithm	xxxii
3.3	Simulation Results	xxxii

<i>TABLE OF CONTENTS</i>	viii
4 Power Allocation in SBD-NOMA	xl
4.1 Proposed Power Allocation	xl
4.1.1 Framed optimization problem	xlii
4.2 Extension to SBD-NOMA with P users in each sub-band . . .	xliv
4.3 Simulation results for the proposed power allocation	xlv
5 Outage Probability in SBD-NOMA	xlvi
5.1 Outage Probability analysis	xlvi
5.2 Approximate PDF of SINR for weak users	xlix
5.3 Approximate PDF of SINR for strong users	li
5.4 Simulation results for the outage probability analysis	liv
6 Conclusions	lvii
A Concavity of Sum rate	lix
A.1 Proof of Lemma 1	lix

List of Figures

1.1	Orthogonal multiple access.	xiv
1.2	Non-Orthogonal multiple access.	xvi
1.3	Comparison between OMA and NOMA.	xvi
3.1	OFDMA vs. NOMA and proposed SBD scheme, $K=24$ for this particular example.	xxvi
3.2	Comparison of sum capacity of OMA, NOMA and proposed SBD scheme.	xxxiv
3.3	Outage probability analysis of SBD-NOMA.	xxxv
3.4	Outage capacity analysis of OMA, NOMA and proposed SBD scheme.	xxxvi
3.5	Impact of cell radius on SBD scheme ($N=2, K=40$).	xxxvii
3.6	Impact of user pairing on SBD scheme.	xxxviii
4.1	Coverage probability comparison of $\text{NOMA}_2, \text{NOMA}_4, K/2$ with different power allocation schemes and NOMA technique.	xlvi
4.2	Outage capacity comparison of $\text{NOMA}_2, \text{NOMA}_4, K/2$ with different power allocation schemes and NOMA technique.	xlvi
5.1	Sum capacity of SBD-NOMA for $K \geq N$	liv
5.2	Outage probability of SBD-NOMA for $K \geq N$	lv

5.3	Outage probability of strong users for $K \geq N$	lv
5.4	Outage probability of weak users for $K \geq N$	lvi
5.5	Comparison of analytical and simulation result for $K \geq N$. . .	lvi

List of Tables

3.1	Percentage Decrease in Sum Capacity by Changing System	
	Bandwidth	xxxviii
3.2	Percentage Increase in Sum Capacity by reducing Path loss	
	Exponent	xxxviii

Chapter 1

Introduction

1.1 Introduction to 5G

From the last few decades wireless communication has undergone very rapid changes. One of the reason for this rapid increase is the way it has affected our lives. Cellular telephony, wifi and other services offered by wireless communicating devices is the major driving force behind all this. The excessive usage of handheld devices for data transmission such as smart phones and tablets is also becoming popular during the last few years, which has motivated the researchers, both in academia and industry, to design the next generation wireless networks. The so-called fifth generation (5G) system will be designed to offer greater spectral efficiency as compared to the conventional fourth generation (4G) systems. Its the future of connectivity. Its something which promise to meet the overwhelming demand of data traffic in 2020 and beyond. However, there are multiple challenges still associated with this field. In order to overcome these challenges there is a need to do extensive work in exploring new techniques, technologies and ideas that can improve the reliability, spectral efficiency and other parameters of

significant importance [1], [2]. In order to do this, 5G systems provide a multitude of techniques to be used in future cellular systems including massive multiple-input multiple-output (MIMO), heterogeneous and small cell networks, millimeter wave (mmWave) communications and other multiple access schemes. The work in this dissertation deals with the novel concept of non-orthogonal multiple access (NOMA), a technique that is considered as a promising enabler towards the 5G of wireless networks.

1.2 Multiple Access Schemes

Traditionally, the multiple access schemes have been broadly classified into two types, i.e., orthogonal multiple access (OMA) and NOMA. The basic difference lies in the way resources are allocated to the users [3].

1.2.1 Orthogonal multiple access

An orthogonal scheme permits a seamless receiver to completely separate unsolicited signals from the desired signal using different basis functions, i.e., signals from separate users are orthogonal to one another in orthogonal schemes. Time division multiple access (TDMA) and orthogonal frequency-division multiple access (OFDMA) are the examples of OMA schemes. In 4G wireless networks, the OMA is mainly based on OFDMA [4]. OFDMA assigns each tone to at most one user such that each user gets disjoint set of subcarriers. Thus, each user experiences a different channel gain on each sub-carrier. The transmitter of OFDMA systems can dynamically allocate power and rate on each tone to satisfy various quality of service (QoS) requirements of each user. The transmitter has the knowledge of perfect channel state information (CSI), which is required in multi-user communication systems.

Thus, OMA techniques such as OFDMA and single carrier frequency division multiple access (SC-FDMA) have been adopted in various systems such as long term evolution (LTE) and LTEadvanced but all these techniques are user oriented and offer lack of user fairness. OMA, being widely used in 4G networks, has no cross correlation and requires simple single user detection but it has low data rates and often sensitive to frequency offset and thus failed to achieve the system upper bound. These schemes are a reasonable choice for achieving good system-level throughput performance in packet-domain services. However, considering the future radio access in the 2020 and beyond, further enhancement to achieve significant system throughput and user fairness has become one of the key issues in handling this explosive data traffic increase in 5G mobile communication systems and need for enhanced delay-sensitive high-volume services. To accommodate these demands, NOMA is considered as a novel and promising candidate for future system enhancement. A topic discussed below.

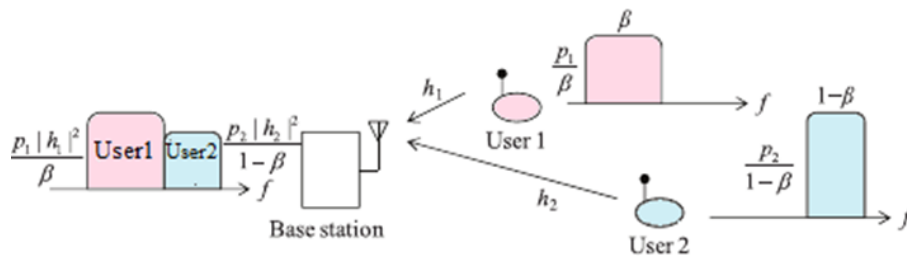


Figure 1.1: Orthogonal multiple access.

1.2.2 Non-Orthogonal multiple access

NOMA, a candidate multiple access scheme for 5G wireless networks because of its ability to share space resource among multiple users in addition to other

benefits being offered. By virtue of this property, NOMA provides higher spectral efficiency, reduced latency, massive connectivity, ultra-fast speeds and user fairness as compared to its orthogonal counterpart [5], [6]. The key feature of NOMA is to explore the multiplexing gain in power domain. In NOMA, the signals from multiple users are superimposed in the power domain in such a way that they offer greater spectral efficiency. Contrary to the conventional water-filling power allocation strategy, the novelty of the NOMA comes from the fact that NOMA technique allocates more transmit power to the users with poor channel conditions (i.e., weak users) and less transmit power to the users with better channel conditions (i.e., strong users). In this case, the weak users can decode their high powered signals directly by treating other signals as noise. In contrast, those users with better channel conditions (i.e., strong users) adopt the successive interference cancellation (SIC) technique for signal detection. In this way, the low powered signals are recovered after SIC [5]. It has been demonstrated that by using superposition coding (SC) together with SIC, both the system throughput and user fairness are significantly improved in NOMA systems compared to conventional OMA systems. However, it requires a rather complex multi-user detection (MUD) at the receiver side especially in massive access scenario. However, by simultaneously allowing multiple users at same frequency/time/code, it achieves the capacity of the Gaussian broadcast channels [4], [6].

1.3 Motivation

As mentioned above, the complexity of MUD is extremely high, especially in massive access scenario. To reduce the complexity, many simplified NOMA schemes have been proposed recently. However, all these schemes are not

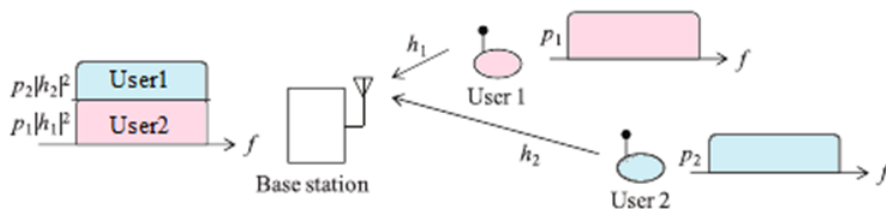


Figure 1.2: Non-Orthogonal multiple access.

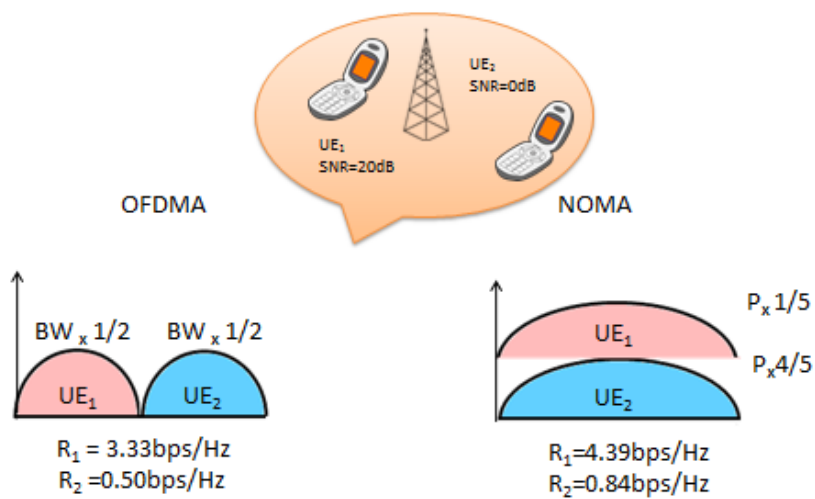


Figure 1.3: Comparison between OMA and NOMA.

capacity-approaching. The primary reason behind this is the simplification of MUD or algorithm used for decoding. On the other hand, the number of practical capacity-approaching schemes proposed in the past are only limited to a few number of users. However, the number of accessed users might be far more than 2 in practical scenarios. Therefore, these capacity approaching techniques cannot be directly adopted. To get high spectrum efficiency, high order inputs are also required. Hence, more complicated techniques are required for decoding users' signal. The optimal approach for uplink (UL) NOMA is to allocate power on the basis of instantaneous channel gain and to share space resource among all the available users [5]. However, in the unconstrained NOMA scheme, there is no upper limit over the number of users that share each subcarrier, which makes the MUD at the receiver a bit complicated. This problem can be mitigated by imposing an upper-limit on the number of users per resource to reduce the receiver complexity [6]. Therefore, in this thesis, to achieve the throughput gain of NOMA with capacity-approaching techniques, we propose an algorithm successive bandwidth division (SBD) in which the users are divided into orthogonal groups with limited number of users in each group. Because of the orthogonality among the users, no joint processing is required at the receiver side to retrieve the users signals. In order to further reduce the inter-set interference, the users within the same sub-band are paired. The users paired within the same sub-band are members of two distinct sets, namely strong set and weak set. The sets are classified on the basis of the channel conditions. The members of weak set should be chosen in a way that it offers very little or no interference to the other user within the same sub-band. As the proposed system is formed by combining OMA and NOMA techniques, so it inherits the advantages of both techniques.

1.4 Problem Statement

To achieve throughput gain of NOMA with practical capacity-approaching techniques and reduced complexity at the receiver and to evaluate the performance gap between SBD-NOMA, OMA and NOMA. To analyze and quantify the effects of power allocation on the performance of UL SBD-NOMA and to provide the closed-form expressions for the probability density function (PDF) of signal-to-interference plus noise ratio (SINR) to calculate the outage for zero forcing (ZF) postcoded receivers.

1.5 Thesis Contribution

The main contributions of this thesis can be listed as:

- We first consider an OFDMA-based MIMO-NOMA UL scenario, known as SBD-NOMA, with constant set of power allocation coefficients. The performance of this proposed SBD-NOMA is characterized with conventional OMA by using the criteria of sum capacity and outage probability.
- An approach to perform the optimal power allocation coefficients for SBD-NOMA with transmission power constraint is proposed. This is because the choice of the power allocation coefficients is a key to achieve a favorable throughput-fairness tradeoff in NOMA systems. Analytical results, such as an exact expressions of power allocation coefficients, are derived for a two user scenario under a total power constraint.
- Under Rayleigh fading, the PDF of the received SINR is approximated by a gamma distribution and closed-form expressions for the outage

probability are presented for SBD-NOMA with no intra-set interference.

1.6 Thesis Organization

The rest of the thesis is organized as follows: Chapter 2 presents the background and existing literature on the leading technology of 5G wireless networks. In chapter 3, we formulate a framework to maximize the outage capacity in SBD-NOMA. Chapter 4 presents a power allocation problem for SBD-NOMA and discuss the optimal solution for two user scenario. Closed-form expressions of outage probability are derived in chapter 5. Chapter 6 generalizes the conclusion drawn from the above frameworks along with the concluding remarks.

Chapter 2

Background and Literature Review

This chapter presents the background and literature review on NOMA.

2.1 NOMA

NOMA has been recognized as a spectral efficient multiple access technique for the next generation of mobile networks. The concept of NOMA can be linked to many previous communication systems. Early works on NOMA system generally consider a transmitter with single antenna. However, it can also be extended to various systems. Ding et al. in [6] study the ergodic sum rate and outage performance of downlink (DL) NOMA. The author considers randomly deployed users with single antenna nodes, which outperform the conventional OMA schemes. Recently, the combination of NOMA is done with MIMO to achieve high spectral efficiency as the application of MIMO to NOMA provides additional degrees of freedom [5]. However, the conventional opportunistic schemes prefer to give all power to the users

with better channel condition, which improves the overall capacity of the system but deteriorates fairness. In [7], the author proposes random opportunistic beamforming for the MIMO NOMA systems, where the base station (BS) transmitter generates multiple beams and superimposes multiple users within each beam. In [8], a ZF-based beamforming and user pairing scheme is proposed for the DL multiuser NOMA system. An UL NOMA transmission scheme is proposed in [9]. Similarly, in [10], the impact of user pairing is characterized by analyzing the sum rates in two NOMA systems. Some other existing work on the design of UL NOMA for 5G wireless network has been proposed in [11], [12] and [13]. The combination of NOMA with cooperative communications and mmWave has been characterized in [14], [15]. Other work on resource allocation in DL NOMA has been characterized in [16]. System level performance of an OFDMA-based NOMA system with fractional transmit power allocation (FTPA) and equal transmit power allocation (ETPA) is considered in [17]. Some other work on power allocation has been discussed in [18], [19]. In [20], the author has presented different power allocation schemes for NOMA considering FTPA, full search power allocation (FSPA) and fixed power allocation (FPA). The FSPA performs well but it has high computational complexity. FPA has worse performance but least complexity. FTPA is a balance between the two but it does not distribute power among the multiplexed users in an optimum way to maximize sum rate.

Chapter 3

Successive Bandwidth Division NOMA system

In this chapter, we present a hybrid suboptimal technique SBD-NOMA, which is an OFDMA-based NOMA system. In SBD-NOMA, the users are orthogonally divided into different sub-bands on the basis of their CSI with limited number of users in each sub-band. Because of the orthogonality among the users, no joint processing is required at the receiver side to retrieve the users' signals. In order to further reduce the inter-set interference, the users within the same sub-band are paired. The users paired within the same sub-band are members of two distinct sets, namely strong set and weak set. The sets are classified on the basis of the channel conditions. The members of weak set should be chosen in a way that they offer very little or no interference to the other users within the same sub-band. As the proposed system is formed by combining OMA and NOMA techniques, it inherits the advantages of both techniques. However, grouping cannot exploit the full potential of NOMA and for that, we perform optimal power allocations. Simulations have shown that this proposed scheme outperforms the OMA

and NOMA scheme by a huge margin.

3.1 System Model

Consider the UL of a multi-user MIMO communication system, where the base station (BS) is equipped with N antennas while the users are equipped with a single antenna each. The total number of users in a cell is K where $K \geq 2N$. The transmission occurs in the presence of additive white Gaussian noise (AWGN) over Rayleigh flat fading channels with path loss. For a conventional UL system with multiple antennas at the BS, only N users can be supported simultaneously without any interference. The novelty of the proposed UL scheme is that, the BS can support $2N$ randomly deployed users at any given instance by SC. Let ξ denotes the set of all K users. In a conventional NOMA scheme, the set ξ is divided into two sets A and B , such that $A \cup B = \xi$ and $A \cap B = \phi$. The sets A and B are defined on the basis of the channel gains that the users experience. In this paper, the term ‘set’ refers to N randomly deployed users chosen on the basis of the channel gains. The sets are classified as *strong* if the corresponding channel gains are large and *weak* if the corresponding channel gains are small, respectively. The sets are determined by sorting the channel gains in descending order and then dividing the channel gains into two halves. The sets thus formed are assumed to be mutually exclusive.

For the case of conventional OMA, the channel is divided into K identical sub-bands to allow access from K different users. All the users are allocated separate frequency bands and the other users cannot use the frequency band other than the one allocated to them. Hence the signals can be decoded independently at the receiver side and ideally no interference arises. However,

the bandwidth assigned to each user is reduced to $1/K$ in this case, which reduces the overall spectral efficiency of the OMA system. In conventional NOMA systems, the users are squeezed in the same frequency band. In this particular case, users in both the sets A and B are allocated to the same frequency band. As multiple users are admitted at the same frequency, the interference offered to them by other users within the sub-band is quite high. We will show later that the users in set B are a constant source of inter-set interference to the users in set A . Thus, the signals of the users in the strong set are decoded first with interference, and then the user signals in the weak set are decoded without interference. As a result, the decoding complexity at the receiver side is very high even aided by SIC or joint decoding. However, for both extremes, it can be seen that the capacity and reliability are affected for OMA and NOMA schemes, respectively. A possible alternative to reduce the interference, receiver complexity, outage probability and to enhance the sum capacity, is to use the proposed SBD-NOMA described in the following section.

3.1.1 Proposed SBD Scheme

The SBD scheme divides the available bandwidth W , of K users, into K/P identical orthogonal sub-bands, each having a bandwidth of W_{sb} . Here P denotes the maximum number of users that can share a sub-band, where $\{P \in \mathbb{N} \mid 1 \leq P \leq K\}$ and \mathbb{N} is a set of natural numbers. The number P leads to the formation of sub-bands with different bandwidths, depending on its value. The superposition of relatively small number of users in each sub-band reduces the receiver complexity and simple user detection techniques can be applied at the receiver side. The P users paired within the same sub-band are chosen from two mutually exclusive sets A and B whose channel

coefficients are pairwise orthogonal.

To get some more insight, consider Fig. 3.1, where the concept of SBD-NOMA is demonstrated. Let the total number of users $K = 24$. For subsequent discussion in this thesis, we define a set ϕ , which is the set of the factors of K . For $K = 24$, $\phi = \{1, 2, 3, 4, 6, 8, 12, 24\}$. Since, the users paired within each sub-bands are assumed to be equal, hence all even elements from ϕ are chosen except $P = 1$. Note that when $P = 1$, conventional OMA scheme works for each sub-band and when $P = K$, the SBD scheme specializes to conventional NOMA. For $P = 2$, the access scheme is denoted as NOMA₂, where the number of users in each sub-band is 2 while the total sub-bands are 12. The number P further divides the strong and weak sets A and B into K/P smaller sets such that $\sum_{m=1}^{K/P} A_m \cup B_m = \xi$, where ξ is a set of all K users and m being the sub-band index. Each A_m and B_m from the sets A and B has a cardinality of 1 for $P = 2$ while there is a single interferer in this case. Similarly, for $P = 4$, SBD-NOMA has 4 users in each sub-band. Each A_m and B_m from the sets A and B has cardinality of 2, whereas the number of interferers is 3 in this case. $P = K$ specializes to the case of conventional UL NOMA, with only one sub-band and $(K - 1)$ interferers. In other words, we define NOMA _{P} to be the access scheme where K/P sub-bands are formed with P users in each sub-band and a conventional NOMA scheme works in each of sub-band.

The number P will affect the number of sub-bands, interferers, dimensions of channel and detection matrices, dimensions of received signal and the number of users in each sub-band. However, the total number of users remains the same. As only P users can transmit their signals at any given instance, hence the received signal is the superposition of the signals from P users. The remaining users are orthogonal. Therefore, in the proposed UL

SBD scheme, the decoding complexity is $O(|\chi|^P)$, while that of conventional NOMA with K users is $O(|\chi|^K)$, where χ denotes the constellation alphabet. However, dividing the entire bandwidth into sub-bands cannot exploit the full potential of NOMA, where all users can occupy the entire bandwidth. Therefore, to cope with this we perform optimal power allocation in SBD-NOMA, which provides an achievable rate much better than the one achieved by without power allocation.

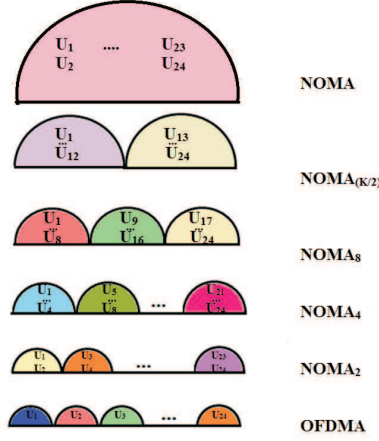


Figure 3.1: OFDMA vs. NOMA and proposed SBD scheme, $K=24$ for this particular example.

3.1.2 Received Signal Model for proposed UL SBD-NOMA

Let's denote the channel matrices of strong and weak sets as \mathbf{H}_1 and \mathbf{H}_2 , respectively, written as

$$\mathbf{H}_1 = \begin{bmatrix} \mathbf{h}_{1,1} & \mathbf{h}_{1,2} & \dots & \mathbf{h}_{1,P/2} \end{bmatrix}, \mathbf{H}_2 = \begin{bmatrix} \mathbf{h}_{2,1} & \mathbf{h}_{2,2} & \dots & \mathbf{h}_{2,P/2} \end{bmatrix}, \quad (3.1)$$

where $\mathbf{h}_{1,j}$ and $\mathbf{h}_{2,n}$ denote the $(N \times 1)$ UL channel vectors of the j^{th} strong and n^{th} weak user, respectively, and are drawn from the complex Gaussian distribution with zero mean and unit variance. The channel vectors are Rayleigh flat faded with path loss. Thus, in the given scenario, the superimposed signal received by the entire group of P users, multiplexed on the m^{th} sub-band, where $1 \leq m \leq K/P$, is given by

$$\mathbf{y} = (\mathbf{H}_1 \mathbf{s}_1 + \mathbf{H}_2 \mathbf{s}_2) + \mathbf{n}, \quad (3.2)$$

where \mathbf{y} is an $(N \times 1)$ UL received signal vectors, $\mathbf{s}_1 = [\sqrt{\alpha_{1,1}}x_{1,1} \sqrt{\alpha_{1,P/2}}x_{1,P/2}]^{\top}$ and $\mathbf{s}_2 = [\sqrt{\alpha_{2,1}}x_{2,1} \dots \sqrt{\alpha_{2,P/2}}x_{2,P/2}]^{\top}$ are $(P/2 \times 1)$ signal vectors of strong and weak sets, respectively. Here, $(\cdot)^{\top}$ denotes the transpose, $\alpha_{i,j}$ represents the NOMA power allocation coefficient of strong and weak users and $x_{i,j}$ represents the symbol transmitted by the j^{th} user to the BS with N antennas and i represents being a member of strong or weak set. The \mathbf{n} is an $(N \times 1)$ AWGN vector, where each value is a normal random variable with zero mean and unit variance. The total number of signals received by the BS is K/P and it depends on the number of users within a particular sub-band.

The received signal of an n^{th} strong user, chosen from the set J , where $J = \{1, 2, \dots, P/2\}$ and $n \in J$ is the superimposed signal given by

$$\mathbf{y}_n = \mathbf{h}_{1,n} \sqrt{\alpha_{1,n}} x_{1,n} + \sum_{j=1}^{P/2} \mathbf{h}_{2,j} \sqrt{\alpha_{2,j}} x_{2,j} + \mathbf{n}, \quad (3.3)$$

where $\mathbf{h}_{1,n}$ and $\mathbf{h}_{2,n}$ are the $(N \times 1)$ UL channel vectors of the n^{th} user from both strong and weak sets to the BS having N antennas and \mathbf{n} is the $(N \times 1)$ AWGN vector.

Since the BS receives superimposed signals, an SIC scheme is required at the receiver side for decoding, the signals of the strong set are decoded

first, with interference from weak set, while the users in the weak set are free from inter-set interference. The remaining users are orthogonal and offer no inter-set interference.

As this thesis assumes perfect CSI, a ZF postcoded or detection matrix is used to decode the signals of strong and weak sets. The corresponding postcoding matrix \mathbf{Z}_i is given by

$$\mathbf{Z}_i = \begin{bmatrix} \mathbf{z}_{i,1}^\top & \mathbf{z}_{i,2}^\top & \cdots & \mathbf{z}_{i,P/2}^\top \end{bmatrix}^\top = (\mathbf{H}_i)^* ((\mathbf{H}_i)(\mathbf{H}_i)^*)^{-1}. \quad (3.4)$$

In the above equation, \mathbf{Z}_1 is the $(P/2 \times N)$ postcoded matrix of users in the strong set and $\mathbf{z}_{i,j}$ is the $(1 \times N)$ vector corresponding to the ZF UL channel vector of the j^{th} user, respectively.

3.1.3 Received SINR

In order to determine the SINR of strong and weak users, respectively, we apply the postcoded matrix \mathbf{Z}_1 to decode the users of strong set, where the received signal vector $\mathbf{r}^{(1)} = [r_{1,1}, r_{1,2}, \dots, r_{1,P/2}]$ becomes

$$\mathbf{r}^{(1)} = \mathbf{Z}_1 \mathbf{y} = \mathbf{Z}_1 \mathbf{H}_1 \mathbf{s}_1 + \mathbf{Z}_1 \mathbf{H}_2 \mathbf{s}_2 + \mathbf{Z}_1 \mathbf{n}, \quad (3.5)$$

where $\mathbf{r}^{(1)}$ is an $(N/(K/P) \times 1)$ received signal vector. From (3.5), the signal of the n^{th} user in the strong set, chosen from the set J , where $n \in J$ is as follow

$$r_{1,n}^{(1)} = \mathbf{z}_{1,n} \mathbf{h}_{1,n} \sqrt{\alpha_{1,n}} x_{1,n} + \sum_{j=1}^{P/2} \mathbf{z}_{1,n} \mathbf{h}_{2,j} \sqrt{\alpha_{2,j}} x_{2,j} + \mathbf{z}_{1,n} \mathbf{n}. \quad (3.6)$$

The corresponding SINR of an n^{th} strong user is given by

$$SINR_{1,n} = \frac{\|\mathbf{z}_{1,n} \cdot \mathbf{h}_{1,n}\|^2 \alpha_{1,n}}{\sum_{j=1}^{P/2} \|\mathbf{z}_{1,n} \cdot \mathbf{h}_{2,j}\|^2 \alpha_{2,j} + \sigma_n^2}, \quad (3.7)$$

where $\|\cdot\|$ denotes the norm operator and $(\mathbf{a} \cdot \mathbf{b})$ represents the point to point multiplication between any two vectors \mathbf{a} and \mathbf{b} . The $\|\mathbf{z}_{1,n} \cdot \mathbf{h}_{1,n}\|^2 \alpha_{1,n}$ represents the desired signal of n^{th} strong user from the set J while the signal $\sum_{j=1}^{P/2} \|\mathbf{z}_{1,n} \cdot \mathbf{h}_{2,j}\|^2 \alpha_{2,j}$ represents the inter-set interference from weak users. Here, it is assumed that the BS has N antennas and, hence, the resultant channel matrices formed at the BS become square, which removes the intra-set interference from other strong and weak users. In this case, each channel vector and the ZF postcoding vector satisfies the following condition.

$$\mathbf{z}_{1,j} \cdot \mathbf{h}_{1,n} = 0; \forall j \neq n, \quad j \in \{1, 2, \dots, P/2\}, \quad (3.8)$$

However, if it is assumed that the BS is equipped with less than N antennas, then the resultant matrix becomes rectangular and hence, the strong and weak users also encounter interference from other strong and weak users, respectively. Consequently, the strong set is affected by a total interference of I , which can be expanded as,

$$I = \sum_{j=1, j \neq n}^{P/2} \|\mathbf{z}_{1,n} \cdot \mathbf{h}_{1,j}\|^2 \alpha_{1,j} + \sum_{j=1}^{P/2} \|\mathbf{z}_{1,n} \cdot \mathbf{h}_{2,j}\|^2 \alpha_{2,j}, \quad (3.9)$$

and the corresponding SINR becomes,

$$SINR_{1,n} = \frac{\|\mathbf{z}_{1,n} \cdot \mathbf{h}_{1,n}\|^2 \alpha_{1,n}}{I + \sigma_n^2}, \quad (3.10)$$

where $\sum_{j=1, j \neq n}^{P/2} \|\mathbf{z}_{1,n} \cdot \mathbf{h}_{1,j}\|^2 \alpha_{1,j}$ represents the intra-set interference from the

other strong users, respectively.

For decoding of weak user signal, SIC is carried out so there will be no interference in this case. Hence, after applying ZF matrix, the signals of weak set become

$$\mathbf{r}^{(2)} = \mathbf{Z}_2 \mathbf{H}_2 \mathbf{s}_2 + \mathbf{Z}_2 \mathbf{n}, \quad (3.11)$$

The received signal and corresponding SINR of n^{th} weak user chosen from the set J , becomes

$$r_{2,n}^{(2)} = \mathbf{z}_{2,n} \mathbf{h}_{2,n} \sqrt{\alpha_{2,n}} x_{2,n} + \mathbf{z}_{2,n} \mathbf{n}, \quad (3.12)$$

$$SINR_{2,n} = \frac{\|\mathbf{z}_{2,n} \cdot \mathbf{h}_{2,n}\|^2 \alpha_{2,n}}{\sigma_n^2}. \quad (3.13)$$

In case of intra-set interference,

$$SINR_{2,n} = \frac{\|\mathbf{z}_{2,n} \cdot \mathbf{h}_{2,n}\|^2 \alpha_{2,n}}{\sum_{j=1, j \neq n}^{P/2} \|\mathbf{z}_{2,n} \cdot \mathbf{h}_{2,j}\|^2 \alpha_{2,j} + \sigma_n^2}. \quad (3.14)$$

The rate of strong and weak user in SBD-NOMA across any sub-band is given by

$$R_{im} = W_{sb} \sum_{j=1}^{P/2} \log_2 (1 + SINR_{i,j}); \quad i \in \{1, 2\}, \quad (3.15)$$

wherein W_{sb} is the sub-band bandwidth.

The summation of P users over all sub-bands m is K , where $K \in \xi$ is the total number of users and it belongs to the set ξ . In other words, we can say

that $n \in J \wedge J \in \xi$. The total sum rate of the system is given by

$$R_{sum} = \sum_{m=1}^{K/P} R_{im} \quad i \in \{1, 2\}. \quad (3.16)$$

Finally, the sum capacities of conventional OMA is written as,

$$R_{i,OMA} = W/K \sum_{k=1}^K \log_2 \left(1 + \frac{|\mathbf{z}_{i,k} \mathbf{h}_{i,k}|^2 \alpha_{i,k}}{\sigma_k^2} \right), \quad (3.17)$$

From (3.16), it can be seen that the user power has a direct effect not only on individual user data rate but also on the SINR of other users, which shows the importance of power allocation in SBD-NOMA system.

3.2 Proposed Channel Allocation Algorithm

In the proposed UL SBD-NOMA scheme, both conventional OMA and NOMA techniques are implemented simultaneously, therefore, the question of users selection in a set is important. The grouping is done on the basis of the channel gains between the users. This is because the user pairing has the potential of reducing the complexity at the receiver side. The user pairing strategy affects the overall throughput of the proposed scheme. Careful user pairing not only improves the sum rate, but also has the potential to improve the individual user rates. The grouping is done on the basis of the channel gains between the users. The pairwise orthogonal users are grouped together in the same sub-band to get full benefit of the NOMA within each sub-band. The detailed algorithm for choosing the members of strong and weak set is presented in Algorithm 1. The algorithm aims to minimize the interference offered by the weak users to the strong users.

The detailed algorithm for choosing members of strong and weak set is presented in Algorithm 3.1. The algorithm aims to minimize the interference offered by the weak user to the strong user.

In step 5 of the above algorithm, the user pairing is critical. It will affect the overall sum capacity of the proposed SBD scheme. This is because the performance of SBD is much dependent on the way the users are paired. Careful user pairing not only improves the sum rate, but also has the potential to improve the individual user rates.

3.3 Simulation Results

In this section, computer simulations are used to evaluate the performance of the proposed SBD-NOMA schemes. We investigate the performance of the SBD schemes and compare it with the conventional OMA and NOMA techniques. The cell radius is assumed to be 1000m in which all the users are randomly distributed. The channel coefficients are assumed to be independent and identically distributed (i.i.d) Rayleigh flat faded. The transmission power allocated to all users is 24dBm. The noise is assumed to be zero mean circular-symmetric complex Gaussian having a noise density of -174dBm/Hz . The overall system bandwidth is 4.32MHz. The path loss is calculated by using the following model

$$PL_{dB} = 30 + 10\beta \log_{10}(d), \quad (3.18)$$

where d is the distance between the BS and the MS and β is the path loss exponent, which is kept at 4 in this study. The working SNR is assumed to be 10dB .

We have compared our proposed scheme with OMA and NOMA schemes.

Algorithm 3.1 Strong and Weak Sets Formation and Subchannel Allocation Algorithm

Initialization

- 1) A set ξ of K users, where $K = \{1, \dots, k\}$.
- 2) \mathbf{H}_1 and \mathbf{H}_2
- 3) Number of antennas, N .

Iteration

- 1) All K users feedback their CSI to the BS. The BS creates a set M of channel matrix, $\mathbf{M} = \{\mathbf{h}_1, \mathbf{h}_2, \dots, \mathbf{h}_k\}$.
- 2) The transmitter then calculates the frobenius norm of all users and arrange it in descending order.

$$M_{ord} = \{|\mathbf{h}_1|^2, |\mathbf{h}_2|^2, \dots, |\mathbf{h}_k|^2\} \text{ where } |\mathbf{h}_k|^2 > |\mathbf{h}_{k+1}|^2 \text{ and } K \in \{1, 2, \dots, k\}.$$

- 3) The transmitter then separates two sets \mathbf{H}_1 and \mathbf{H}_2 from M_{ord} on the basis of the channel gains that the user experience i.e., $\mathbf{H}_1 \cup \mathbf{H}_2 = M_{ord}$ and $\mathbf{H}_1 \cap \mathbf{H}_2 = \phi$.

$$\begin{aligned} \mathbf{H}_1 &= \{|\mathbf{h}_1|, |\mathbf{h}_2|, \dots, |\mathbf{h}_{\lfloor K/2 \rfloor}|\}, \\ \mathbf{H}_2 &= \{|\mathbf{h}_{\lfloor K/2 \rfloor + 1}|, |\mathbf{h}_{\lfloor K/2 \rfloor + 2}|, \dots, |\mathbf{h}_k|\}, \end{aligned}$$

$\lfloor \cdot \rfloor$ denotes the floor function. In \mathbf{H}_1 , the N users having the higher channel gains are selected as the members of strong set A , while the remaining users are selected as the members of the weak set, B . The respective channel gains of strong and weak users are \mathbf{H}_1 and \mathbf{H}_2 . The users with channel gains \mathbf{H}_1 are members of set A and users with channel gains \mathbf{H}_2 are members of set B .

$$\begin{aligned} \mathbf{H}_1 &= \begin{bmatrix} \mathbf{h}_{1,1} & \mathbf{h}_{1,2} & \dots & \mathbf{h}_{1,N} \end{bmatrix}^T, \\ \mathbf{H}_2 &= \begin{bmatrix} \mathbf{h}_{2,1} & \mathbf{h}_{2,2} & \dots & \mathbf{h}_{2,N} \end{bmatrix}^T, \end{aligned}$$

- 4) Do head to tail pairing of users from both sets to get minimum interference.
- 5) For SBD NOMA, each Rayleigh fading channel matrix divides itself into smaller matrices with dimension $N \times P/2$, where P denotes the access scheme. The smaller channel matrices and the corresponding user indexes of strong and weak sets satisfy the condition $\sum_{i=1}^{K/p} A_i \cup B_i = \xi$. The users from the two sets are paired in different sub-bands to reduce interference. Go to 1).

End When all the N users from the two sets are paired in sub-bands.

The first comparison is done in terms of sum capacity with a constant set of power allocation coefficients. On the other hand, the second comparison is done in terms of outage probability analysis. Furthermore, the effect of cell radius is also taken into account in 3.4.

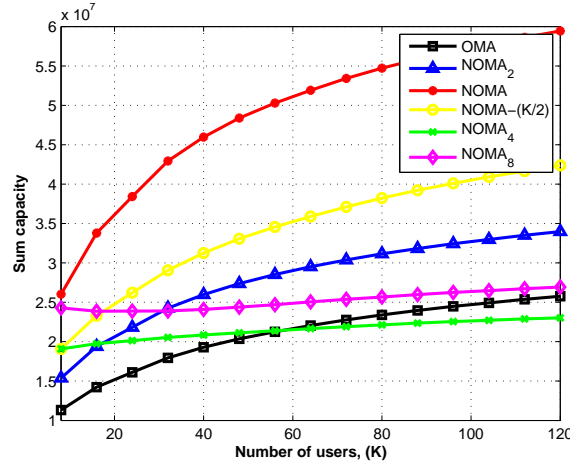


Figure 3.2: Comparison of sum capacity of OMA, NOMA and proposed SBD scheme.

Fig. 3.2 demonstrates the relationship between sum capacity and varying the number of users, K. The figure compares the sum capacity of OMA, NOMA and proposed SBD-NOMA schemes each having a fixed set of power allocation coefficients. The primary observation of this section is comparing the sum capacity of all multiple access schemes with the number of users and examining the effect of number of users. The sum capacity improves with the increase in the number of users but that improvement is not substantial for NOMA₄ and NOMA₈ schemes after the number of users exceeds a certain limit, because of significant interference. However, these schemes offer better coverage probability and hence their outage probability is quite low and they offer less complexity than the conventional NOMA technique. The inconsistency in performance is because of the reason that SBD-NOMA can

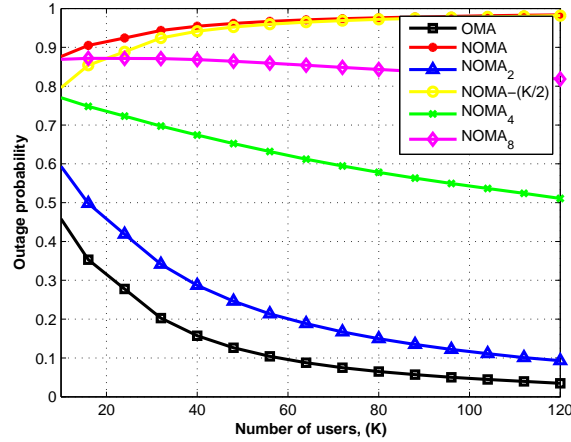


Figure 3.3: Outage probability analysis of SBD-NOMA.

reduce the achievable rates as dividing the entire bandwidth into sub-bands cannot exploit the full potential of NOMA, where all users can occupy the entire bandwidth. As bandwidth is directly proportional to each user's data rate, the effect is visible in the sum capacity analysis. However, dividing the users into orthogonal groups will reduce the intra-set interference. The major outcome of sharing is that the sum rate is expected to improve, which can be further enhanced by properly allocating power to weak users. Also it can be noticed that OMA techniques have a very poor spectrum fairness index among the users. This is because there is exclusivity in resource allocation, i.e., a resource block allocated to one user can not be used by any other user. However, the fairness offered by SBD-NOMA is way better than OFDMA with reduced complexity and signaling overhead at the BS. However, the complexity offered by them is much less than the conventional UL NOMA system. The $\text{NOMA}_{K/2}$ scheme outperforms the OMA and conventional NOMA techniques in terms of receiver complexity, decoding and offer better throughput and fairness.

Fig. 3.3 shows the outage performance of OMA, NOMA and proposed

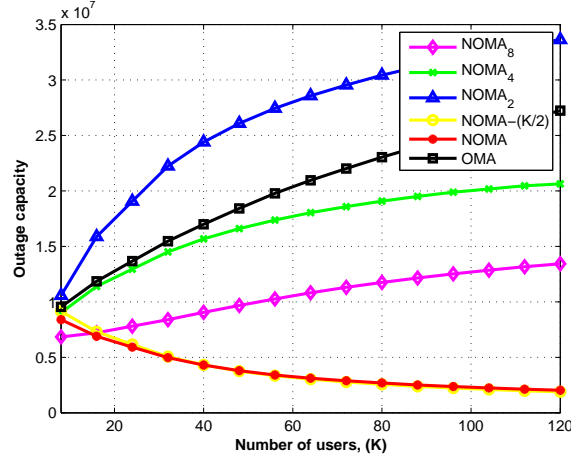


Figure 3.4: Outage capacity analysis of OMA, NOMA and proposed SBD scheme.

SBD schemes. It can be easily observed that the proposed SBD schemes can achieve better outage performance as compared to conventional NOMA especially NOMA₂ and NOMA_{K/2} schemes. The decreasing trend of outage probability in SBD scheme is because of the fact that we are dividing the bandwidth and noise variance accordingly which increases the individual SINR of users. As a result, the rate offered by conventional OMA is minimum but its outage probability is low, which increases the overall outage capacity of the conventional OMA system. The outage capacity is defined as the maximum rate that can be maintained by each user multiplied with the success probability of the users. It shows a clear picture of system performance for both data rates and success of each user. The outage capacity analysis of SBD-NOMA is evaluated in 3.4. SBD-NOMA performs well in terms of outage capacity as shown. We can derive an interesting result by combining Fig. 3.2 and 3.3 that although the conventional UL NOMA achieves maximum sum capacity but it increases the receiver complexity and outage probability to a great extent, which is practically not desired especially if the

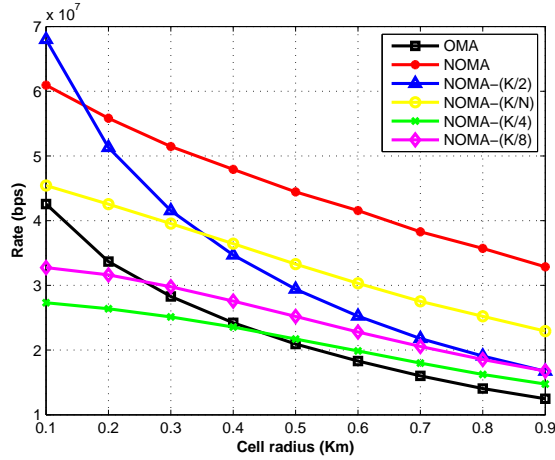


Figure 3.5: Impact of cell radius on SBD scheme ($N=2$, $K=40$).

number of users is very large. Hence in the situations where the user priority is reduced complexity, cost and enhanced QoS, SBD-NOMA schemes should be preferred over conventional UL NOMA, which provide better rate and a fairly reliable transmission scheme.

In Fig. 3.5, the impact of cell radius on the performance of OMA, NOMA and SBD-NOMA is demonstrated. It can be seen that SBD-NOMA performs better than the conventional NOMA if the cell radius is assumed to be very small. However, NOMA outperforms at other values, but as the cell radius increases, the inter-set interference offered to NOMA by weak set also enhances, which increases the decoding complexity at the receiver side.

Fig. 3.6 shows the effect of user pairing in SBD-NOMA. It can be seen that the user pairing affects the overall sum rate of the system. Different user pairing strategies have been discussed in the literature. The best performance occurs by pairing users head to tail. This is because of minimum inter-set interference. The same trend is shown in the figure.

Finally, the effect of changing system bandwidth and path loss exponent on the performance of SBD-NOMA has been evaluated for $K = 40$. De-

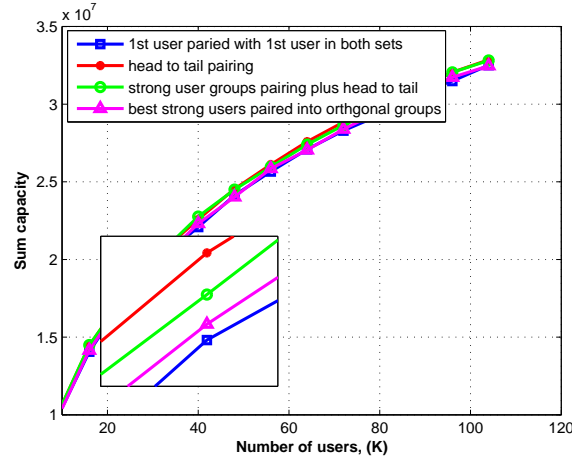


Figure 3.6: Impact of user pairing on SBD scheme.

Table 3.1: Percentage Decrease in Sum Capacity by Changing System Bandwidth

System Bandwidth	OMA	NOMA	NOMA-(K/2)
2.16 MHz	39.1 %	45.7 %	39.7 %
1.08 MHz	63.90 %	70.50 %	64.80 %
System Bandwidth	NOMA-(K/N)	NOMA-(K/4)	NOMA-(K/8)
2.16 MHz	43.10%	42.14 %	41.25 %
1.08 MHz	67.60 %	67.20 %	66.72 %

Table 3.2: Percentage Increase in Sum Capacity by reducing Path loss Exponent

Path loss Exponent	OMA	NOMA	NOMA-(K/2)
3.76	34.1 %	41.9%	29.2 %
3.1	70 %	59.0 %	58.7 %
Path loss Exponent	NOMA-(K/N)	NOMA-(K/4)	NOMA-(K/8)
3.76	27.9%	27.3 %	18 %
3.1	57.39%	46.9 %	39.7 %

creasing the system bandwidth to 2.16MHz and 1.08MHz reduces the sum capacity as compared to 4.32MHz. The percentage decrease for each SBD-NOMA scheme is shown in Table 3.1. Reducing the system bandwidth to one half almost decreases the sum capacity to 40% for each scheme. Similarly,

decreasing the system bandwidth to one quarter reduces the sum capacity in a range of 60 to 70%. The percentage decrease in sum capacity is highest for NOMA, as the number of interferers is large for NOMA. Similarly, decreasing the path loss exponent increases the sum capacity as shown in Table 3.2. The percentage increase in sum capacity is not substantial for NOMA₈ scheme. However, it can be observed that NOMA₂ dominates NOMA _{$K/2$} at path loss exponent of 3.1.

Chapter 4

Power Allocation in SBD-NOMA

In this chapter, we perform optimal power allocation to improve the performance of the proposed MIMO-NOMA system.

4.1 Proposed Power Allocation

In the previous chapter, constant power allocation coefficients are considered. However, dividing the users into orthogonal groups cannot exploit the full potential of NOMA with the exception that the complexity at the receiver side is reduced. Therefore, more sophisticated choices of power allocation are considered in this chapter. It is worth pointing out that optimizing power allocation according to instantaneous channel conditions further improves the performance of MIMO-NOMA system. This leads to the formation of SBD-NOMA system with optimal power allocation. The main purpose is to maximize the sum rate across all sub-bands by allocating optimal power and also provide some degree of fairness to each user. The corresponding

resource allocation problem considers the number of users in each sub-band, the choice of user pairing and the power allocated to each sub-band. The framed optimization problem maximizes the sum rate while also ensures fairness in the system. For the sake of simplicity, we are assuming two users in each sub-band while the total number of users is K . Instead of allocating power values to each sub-band through iterative water filling, the power allocated across each sub-band is assumed to be equally allocated, which would reduced the signaling overhead and complexity of the proposed numerical solutions. However, in general, the sum rate is not convex in nature for more than two transmitting sources, hence, the solution is proposed here for NOMA₂. The numerical solution for other schemes is not proposed here due to duality gap in transformation from non-convex to convex function.

Lemma 1: The achievable sum rate of the system is concave in nature for more than two transmitting sources.

Proof: See Appendix A.

Mathematically, the problem is formulated as

$$\begin{aligned}
 & \underset{\alpha_{i,j}}{\text{maximize}} && R_{im} \\
 & \text{subject to} && \alpha_{1,j} + \alpha_{2,j} \leq P_T, \forall j \\
 & && \alpha_{i,j} \geq 0, \forall i, \forall j \\
 & && R_{im,j} \geq r_{min}, \text{ where } j \in J,
 \end{aligned} \tag{4.1}$$

where (4.1) represents the constraints of the framed optimization problem, P_T is the total power allocated to users within a particular sub-band, R_{im} represents the data rate across each sub-band, $R_{im,j}$ represents the individual data rate of j^{th} user and r_{min} represents the minimum target rate to maintain fairness among the users. The users are already paired and are chosen from

two distinct sets to reduce the inter-set interference, where

$$\sum_{j=1}^{P/2} \alpha_{i,j} = P_T, \forall i. \quad (4.2)$$

4.1.1 Framed optimization problem

Taking into account the objective function described above and solving the optimization problem through Lagrange multipliers leads to the following formulation of the objective function denoted by F , i.e.,

$$F = R_{im} + \sum_{j=1}^{P/2} \lambda_j (P_T - \alpha_{1,j} - \alpha_{2,j}) + \sum_{j=1}^{P/2} \kappa_j (R_{1m,j} - r_{min}) + \sum_{j=1}^{P/2} \tau_j (R_{2m,j} - r_{min}), \quad (4.3)$$

where λ_j , κ_j and τ_j represent the Lagrange multipliers. Using the standard procedure, by differentiating F with respect to all $\alpha_{1,j}$ and $\alpha_{2,j}$ and by setting them equal to zero, we obtain a non-linear system of $5|J|$ equations having $5|J|$ unknowns, where $|J|$ denotes the cardinality of set J . For the sake of simplicity, the derivatives here are taken only for $\alpha_{1,j}$, $\alpha_{2,j}$, τ_j , λ_j and κ_j . A similar procedure can be used for other variables as well. The entire procedure is repeated over all sub-bands to maximize the overall sum rate.

We obtain

$$\begin{aligned} \partial F / \partial \alpha_{1,j} = & \frac{W_{sb} \|\mathbf{z}_{1,j} \cdot \mathbf{h}_{1,j}\|^2}{\|\mathbf{z}_{1,j} \cdot \mathbf{h}_{2,j}\|^2 \alpha_{2,j} + \sigma_j^2 + \|\mathbf{z}_{1,j} \cdot \mathbf{h}_{1,j}\|^2 \alpha_{1,j}} - \lambda_j \\ & - \kappa_j \frac{W_{sb} \|\mathbf{z}_{1,j} \cdot \mathbf{h}_{1,j}\|^2}{\|\mathbf{z}_{1,j} \cdot \mathbf{h}_{2,j}\|^2 \alpha_{2,j} + \sigma_j^2 + \|\mathbf{z}_{1,j} \cdot \mathbf{h}_{1,j}\|^2 \alpha_{1,j}}, \end{aligned} \quad (4.4)$$

$$\begin{aligned}
\partial F/\partial\alpha_{2,j} = & -\frac{W_{sb}\|\mathbf{z}_{1,j}\cdot\mathbf{h}_{1,j}\|^2\|\mathbf{z}_{1,j}\cdot\mathbf{h}_{2,j}\|^2\alpha_{1,j}}{\|\mathbf{z}_{1,j}\cdot\mathbf{h}_{2,j}\|^2\alpha_{2,j}+\sigma_j^2+\|\mathbf{z}_{1,j}\cdot\mathbf{h}_{1,j}\|^2\alpha_{1,j}\varphi} + \frac{\|\mathbf{z}_{2,j}\cdot\mathbf{h}_{2,j}\|^2}{\|\mathbf{z}_{2,j}\cdot\mathbf{h}_{2,j}\|^2\alpha_{2,j}+\sigma_j^2} \\
& -\lambda_j + \kappa_j \frac{W_{sb}\|\mathbf{z}_{1,j}\cdot\mathbf{h}_{1,j}\|^2\|\mathbf{z}_{1,j}\cdot\mathbf{h}_{2,j}\|^2\alpha_{1,j}}{\|\mathbf{z}_{1,j}\cdot\mathbf{h}_{2,j}\|^2\alpha_{2,j}+\sigma_j^2+\|\mathbf{z}_{1,j}\cdot\mathbf{h}_{1,j}\|^2\alpha_{1,j}\varphi} + \tau_j \frac{W_{sb}\|\mathbf{z}_{2,j}\cdot\mathbf{h}_{2,j}\|^2}{\sigma_j^2},
\end{aligned} \tag{4.5}$$

where $\varphi = \|\mathbf{z}_{1,j}\cdot\mathbf{h}_{2,j}\|^2\alpha_{2,j} + \sigma_j^2$.

$$\partial F/\partial\lambda_j = P_T - \alpha_{1,j} - \alpha_{2,j}, \tag{4.6}$$

$$\partial F/\partial\kappa_j = W_{sb}\log_2\left(1 + \frac{\|\mathbf{z}_{1,j}\cdot\mathbf{h}_{1,j}\|^2\alpha_{1,j}}{\|\mathbf{z}_{1,j}\cdot\mathbf{h}_{2,j}\|^2\alpha_{2,j} + \sigma_j^2}\right) - r_{min}, \tag{4.7}$$

$$\partial F/\partial\tau_j = W_{sb}\log_2\left(1 + \frac{\|\mathbf{z}_{2,j}\cdot\mathbf{h}_{2,j}\|^2\alpha_{2,j}}{\sigma_j^2}\right) - r_{min}, \tag{4.8}$$

$$\alpha_{1,j} \cdot \partial F/\partial\alpha_{1,j} = 0, \tag{4.9}$$

$$\alpha_{2,j} \cdot \partial F/\partial\alpha_{2,j} = 0, \tag{4.10}$$

$$\lambda_j \cdot \partial F/\partial\lambda_j = 0, \tag{4.11}$$

$$\kappa_j \cdot \partial F/\partial\kappa_j = 0, \tag{4.12}$$

$$\tau_j \cdot \partial F/\partial\tau_j = 0, \tag{4.13}$$

where $\alpha_{1,j}, \alpha_{2,j}, \lambda_j, \kappa_j, \tau_j \geq 0$. Solving the above Equation (4.4) for the Lagrange variable λ_j , and substituting it in (4.5) and the value of $\alpha_{2,j}$ from (4.6) gives the value of $\alpha_{1,j}$. The $\alpha_{1,j}$ turns out to be

$$\alpha_{1,j} = \frac{\sqrt{\varphi_{bj}}(-2\varphi_{cj}(r_{min} + \tau_j) + \varphi_{aj}(2r_{min} + \kappa_j + \tau_j)(\varphi_{cj}P_T + \sigma_j^2))}{2\sqrt{(\varphi_{bj})(\varphi_{aj} - \varphi_{cj})\varphi_{cj}(r_{min} + \tau_j)}} - \frac{\sqrt{\varphi_{aj}}\sqrt{(\varphi_{cj}P_T + \sigma_j^2)}\sqrt{\varphi_{aj}\varphi_{bj}\varphi_{cj}P_T(\kappa_j - \tau_j)^2 + \Psi_1 + \Psi_2}}{2\sqrt{(\varphi_{bj})(\varphi_{aj} - \varphi_{cj})\varphi_{cj}(r_{min} + \tau_j)}}, \quad (4.14)$$

where $\Psi_1 = \varphi_{bj}(-4\varphi_{cj}(r_{min} + \kappa_j)(r_{min} + \tau_j) + \varphi_{aj}(2r_{min} + \kappa_j + \tau_j)^2)\sigma_j^2$ and $\Psi_2 = 4\varphi_{cj}(-\varphi_{aj} + \varphi_{cj})(r_{min} + \kappa_j)(r_{min} + \tau_j)\sigma_j^2$. The φ_{aj} , φ_{bj} and φ_{cj} are given by $\varphi_{aj} = \|\mathbf{z}_{1,j} \cdot \mathbf{h}_{1,j}\|^2$, $\varphi_{bj} = \|\mathbf{z}_{2,j} \cdot \mathbf{h}_{2,j}\|^2$, $\varphi_{cj} = \|\mathbf{z}_{1,j} \cdot \mathbf{h}_{2,j}\|^2$.

The value of $\alpha_{2,j}$ is derived by substituting the value of $\alpha_{1,j}$ in (4.6) and is given by

$$\alpha_{2,j} = P_T - \alpha_{1,j}. \quad (4.15)$$

4.2 Extension to SBD-NOMA with P users in each sub-band

To investigate the scenario of more than two users in each sub-band, multistage power allocation is proposed. In the first stage, the users form two distinct sets A and B on the basis of algorithm presented in Algorithm 3.1. After this step, two sub-bands from sets A and B are formed, each having equal number of users. The power allocated to each sub-band is equal to half of the total transmission power. In this scenario, the channel gains become the sum of all channel powers in the two sub-bands. The same procedure for SBD-NOMA₂ is repeated for power allocation within the two sub-bands. In

the second stage, the two sub-bands further divide themselves into smaller sub-bands, i.e., two sub-bands are formed in each sub-band of the previous stage with the total power per sub-band as determined in the first stage. In the third stage, these sub-bands further divide into smaller sub-bands to allocate power to all users. The procedure is repeated until all users are allocated with an optimal transmission power.

4.3 Simulation results for the proposed power allocation

allocation

In these simulation, we plot the results for a UL SBD-NOMA system with proposed power allocation coefficients. The same parameters have been considered as in the previous chapter. We then analyze these results from different perspectives to establish meaningful and valuable insights.

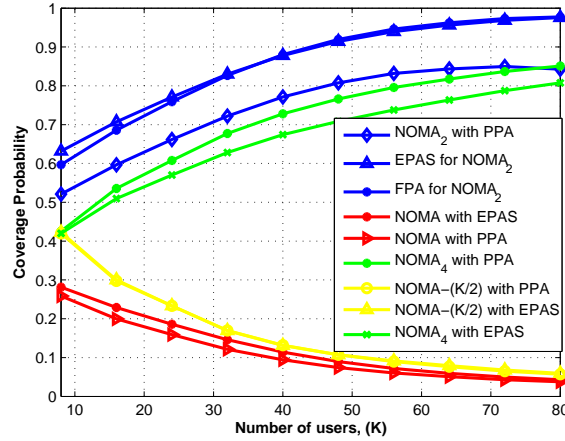


Figure 4.1: Coverage probability comparison of NOMA₂, NOMA₄, $K/2$ with different power allocation schemes and NOMA technique.

Fig.4.1 compares the coverage probability of conventional NOMA and SBD-NOMA with different power allocation schemes. *Coverage probability*

is defined as the probability that a certain number of users achieves a data rate greater than the target data rate, which is taken as 3.34 Mbps in this study. It can be easily seen that SBD-NOMA performs well as compared to NOMA in terms of coverage probability. The coverage probability of FPA and EPAS is even better in this case as compared to the proposed approach, however, EPAS being the simplest criteria of allocating power to users does not perform well, as it allocates equal power to all users and therefore treats the weak users in the same manner as the strong ones. The SBD-NOMA provides every pair a power that suits their channel gain, which allows a balance between the required power, fairness and the target rate with total power allocation constraint across each sub-band. Although, the optimal NOMA scheme shows greater sum rate but its coverage probability in this scenario is less than the optimal solution even after proposed power allocation. The same trend is depicted in the Fig.4.1.

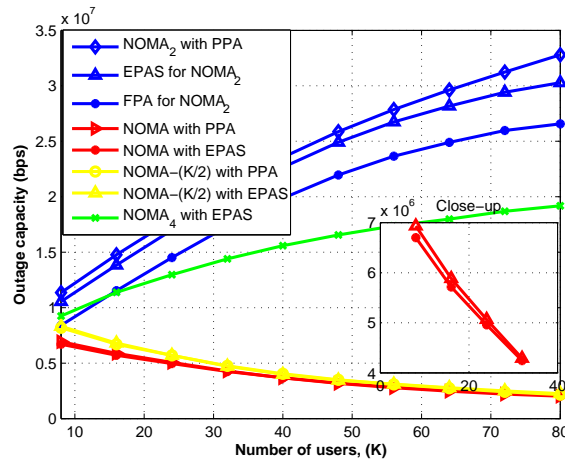


Figure 4.2: Outage capacity comparison of NOMA₂, NOMA₄, $K/2$ with different power allocation schemes and NOMA technique.

Fig. 4.2 shows the outage capacity of SBD-NOMA with conventional NOMA scheme. The outage capacity is larger for SBD-NOMA₂ with the

proposed power allocation scheme. The proposed power allocation in NOMA increases the outage capacity as compared to the NOMA with EPAS but the increase is quite substantial. However, with equal power allocation, the system treats the weak users in the same way as strong users. As strong users get significant interference from weak users, hence, the capacity of strong users gets degraded. The optimal power allocation in SBD-NOMA ensures fairness in the system by imposing an upper limit on each user's individual data rate as compared to EPAS and FPA schemes. The performance margin in NOMA and SBD-NOMA with and without power allocation is quite high in terms of outage capacity. From this figure, it is clear that the proposed power allocation scheme performs better than the existing ones.

Chapter 5

Outage Probability in SBD-NOMA

In this chapter, outage probability of SBD-NOMA is evaluated for a ZF postcoded receiver.

5.1 Outage Probability analysis

The outage probability is an important performance metric as it measures the probability of unsuccessful signal decoding for a given service. The outage probability experienced by any n^{th} user in weak set can be defined as

$$\begin{aligned} P_o &= 1 - Pr(SINR_{2,n} > r_{min}) \\ &= 1 - Pr\left(\frac{|\mathbf{z}_{2,n} \cdot \mathbf{h}_{2,n}|^2 \alpha_{2,n}}{\sigma_n^2} > r_{min}\right), \end{aligned} \quad (5.1)$$

Building on the above Equation (5.1), the outage probability experienced by any n^{th} user in strong set can be written as,

$$\begin{aligned}
P_o &= 1 - Pr(SINR_{1,n} > r_{min}) \\
&= 1 - Pr\left(\frac{\|\mathbf{z}_{1,n} \cdot \mathbf{h}_{1,n}\|^2 \alpha_{1,n}}{\sum_{j=1}^{P/2} \|\mathbf{z}_{1,n} \cdot \mathbf{h}_{2,j}\|^2 \alpha_{2,j} + \sigma_n^2} > r_{min}\right), \tag{5.2}
\end{aligned}$$

In the above expressions, there is no intra-set interference. Here, it is assumed that the BS is equipped with N antennas and, hence, the number of interferers from the weak set are also N , therefore, it may be stated that the strong users are only affected by inter-set interference from the weak users. Furthermore, $\mathbf{Z}_2 \mathbf{H}_2 = \mathbf{I}_k$ and $\mathbf{z}_{2,n} \mathbf{h}_{2,j} = \delta_{nj}$ where $\delta_{nj} = 1$ for $n = j$ and 0 otherwise. The same holds true for the strong users as well. We first derive the approximate PDF of the SINR of the users in strong and weak sets, respectively.

5.2 Approximate PDF of SINR for weak users

To derive the PDF of the SINR of weak users, the SINR given by (3.13), can be written as,

$$SINR_{2,n} = \frac{\alpha_{2,n}}{\sigma_n^2} \triangleq \frac{\alpha_{2,n}}{\|\mathbf{z}_{2,n}\|^2 \sigma^2} \triangleq \frac{\alpha_{2,n}}{[(\mathbf{H}_2^* \mathbf{H}_2)^{-1}]_{nn} \sigma^2}. \tag{5.3}$$

Denoting the SINR defined in (5.3) with a random variable (RV) Y , it becomes

$$SINR_{2,n} = \frac{\alpha_{2,n}}{Y \sigma^2}, \tag{5.4}$$

where $Y = [(\mathbf{H}_2^* \mathbf{H}_2)^{-1}]_{nn}$. From (5.4), it is obvious that we can derive the PDF of SINR provided that the PDF of Y is known. The RV Y in the

denominator of (5.4) is expanded as

$$[(\mathbf{H}_2^* \mathbf{H}_2)^{-1}]_{nn} = \frac{1}{(\mathbf{h}_{2,n})^* \mathbf{h}_{2,n} - (\mathbf{h}_{2,n})^* \mathbf{H}_{2n} (\mathbf{H}_{2n}^* \mathbf{H}_{2n})^{-1} \mathbf{h}_{2,n} (\mathbf{H}_{2n})^*}, \quad (5.5)$$

where \mathbf{H}_{2n} is the sub matrix obtained after removing the n^{th} column from the matrix \mathbf{H}_2 . Hence,

$$SINR_{2,n} = \frac{\alpha_{2,n} (\mathbf{h}_{2,n})^* \mathbf{h}_{2,n} - (\mathbf{h}_{2,n})^* \mathbf{H}_{2n} (\mathbf{H}_{2n}^* \mathbf{H}_{2n})^{-1} \mathbf{h}_{2,n} (\mathbf{H}_{2n})^*}{\sigma^2}. \quad (5.6)$$

Generally, for any $N \times K$ Rayleigh fading matrix, the expression in the numerator of (5.6) follows a gamma distribution with shape parameter $N - K + 1$ and scale parameter 1, i.e., $\Gamma(N - K + 1, 1)$. This is because it represents sum of independent and identically distributed (i.i.d.) exponential RVs each having a unit mean and the PDF is given as

$$f_Y(y) = \frac{y^{(N-K)} \exp(-y)}{\Gamma(N - K + 1)}. \quad (5.7)$$

However, in the above case, there are N users in each set and the channel gains are Rayleigh faded with path loss. Therefore, the expression in the numerator of (5.6) follows a gamma distribution with shape parameter 1 and scale parameter λ_{in} i.e., $\Gamma(1, \lambda_{in})$, where λ_{in} is the mean power experienced by the n^{th} user because of path loss. The $\Gamma(1, \lambda_{in})$, with shape parameter 1 converges to an exponential distribution given by

$$f_Y(y) = \frac{1}{\lambda_{in}} \exp\left(\frac{-y}{\lambda_{in}}\right), \quad (5.8)$$

Multiplication with power allocation coefficient $\alpha_{2,n}$ and division by the noise variance σ^2 , both of which are constants for a particular user will only change the mean parameter of the RV Y . Hence, the final closed-form expression

for the PDF of the SINR of weak user becomes

$$f_Y(y) = \frac{1}{\tau_{in}} \exp\left(\frac{-y}{\tau_{in}}\right), \quad (5.9)$$

where τ_{in} is the modified mean. To calculate the outage, we have

$$Pr(SINR_{2,n} > r_{min}) = \int_{r_{min}}^{\infty} f_Y(y) dy. \quad (5.10)$$

Using (5.1), we obtain the outage probability of weak users.

5.3 Approximate PDF of SINR for strong users

To derive the PDF of SINR of strong users, the SINR given by (3.7) can be written as

$$\begin{aligned} SINR_{1,n} &= \frac{\alpha_{1,n}}{\sum_{j=1}^{P/2} \|\mathbf{z}_{1,n} \cdot \mathbf{h}_{2,j}\|^2 \alpha_{2,j} + \|\mathbf{z}_{1,n}\|^2 \sigma^2} \\ &\triangleq \frac{\alpha_{2,n}}{\sum_{j=1}^{P/2} \|\mathbf{z}_{1,n} \cdot \mathbf{h}_{2,j}\|^2 \alpha_{2,j} + [(\mathbf{H}_1^* \mathbf{H}_1)^{-1}]_{nn} \sigma^2}. \end{aligned} \quad (5.11)$$

Denoting the SINR defined in (5.11) with RV X and T , it becomes

$$SINR_{1,n} = \frac{\alpha_{1,n}}{X + T\sigma^2}, \quad (5.12)$$

where $T = [(\mathbf{H}_1^* \mathbf{H}_1)^{-1}]_{nn}$. To calculate the PDF of the SINR of strong users, we need to calculate the PDF of the RV X and T . The PDF of the product of $T\sigma^2$ is already known from above. To derive the density function of interference represented by X , notice that X is a sum of exponential RVs and its PDF is given by Gamma distribution, i.e.,

$$X = \sum_{j=1}^{P/2} \|\mathbf{z}_{1,n} \cdot \mathbf{h}_{2,j}\|^2 \alpha_{2,j}, \quad (5.13)$$

$$f_X(x) = \frac{x^{(v-1)} \exp(-x/\Omega)}{\Gamma(v)\Omega^v}, \quad (5.14)$$

where $v = \frac{\mathbb{E}[X]^2}{\text{var}[X]}$ and $\Omega = \frac{\text{var}[X]}{\mathbb{E}[X]}$. To derive the analytical expressions for v and Ω , we assume independent interfering signals from weak users, where the power allocation coefficient $\alpha_{2,j}$ is considered as a constant for a particular user. Hence, the mean and variance of X can be written as

$$\mathbb{E}[X] = \sum_{j=1}^{P/2} \alpha_{2,j} \mathbb{E}[W_j], \quad (5.15)$$

where $W_j = \varphi_{cjn} = \|\mathbf{z}_{1,n} \cdot \mathbf{h}_{2,j}\|^2$ and

$$\text{var}(X) = \sum_{j=1}^{P/2} \alpha_{2,j}^2 \text{var}(W_j). \quad (5.16)$$

It can be seen that the PDF of W_j is also gamma distributed with unit scale parameter. The general expression of the PDF for the case $N \geq K$ can be written as,

$$f_W(w) = \frac{K^{N-K+1} \exp(-Kx) w^{N-K}}{\Gamma(N-K)}, \quad (5.17)$$

$$\mathbb{E}(W_j) = 1, \quad (5.18)$$

$$\text{var}(W_j) = 1. \quad (5.19)$$

Therefore, the values of v and Ω are given by

$$v = \frac{(\sum_{j=1}^{P/2} \alpha_{2,j})^2}{\sum_{j=1}^{P/2} \alpha_{2,j}^2}, \quad (5.20)$$

and

$$\Omega = \frac{\sum_{j=1}^{P/2} \alpha_{2,j}^2}{\sum_{j=1}^{P/2} \alpha_{2,j}}. \quad (5.21)$$

Using (5.20) and (5.21), PDF of X can be computed. The PDF of the product $T\sigma^2$ is already known. The addition of two independent gamma random variables is also gamma distributed. The numerator of (5.11) is just a power allocation coefficient $\alpha_{1,n}$, which is considered as a constant, hence, just change the scale parameter of resultant gamma distribution. Therefore, the final expression for the PDF of SINR can be written as

$$f_U(u) = \frac{u^{(s-1)} \exp(-u/\Omega_w)}{\Gamma(s)\Omega_w^s}, \quad (5.22)$$

where s and Ω_w are the resultant shape and scale parameters, respectively.

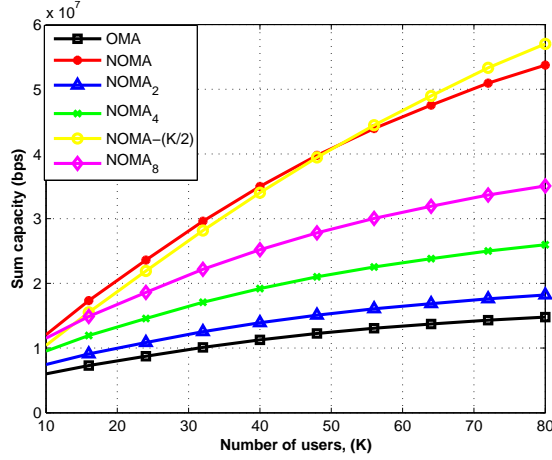
To calculate the outage, we have

$$Pr(SINR_{1,n} > r_{min}) = \int_{r_{min}}^{\infty} \frac{u^{(s-1)} \exp(-u/\Omega_w)}{\Gamma(s)\Omega_w^s} du, \quad (5.23)$$

Equation (5.23) can be expanded as

$$\exp\left(-\frac{r_{min}}{\Omega_w}\right) \sum_{f=0}^s \frac{\left(\frac{r_{min}}{\Omega_w}\right)^f}{f!}. \quad (5.24)$$

By using the above equation, coverage probability can be computed. Hence, by using (5.2), we obtain the outage probability of strong users.

Figure 5.1: Sum capacity of SBD-NOMA for $K \geq N$.

5.4 Simulation results for the outage probability analysis

Fig. 5.1 and 5.2 depict the sum capacity and outage probability of SBD-NOMA with no intra-set interference. It can be observed from the figure that with no intra-set interference, the sum rate is inversely proportional to the number of sub-bands. However, $\text{NOMA}_{K/2}$ nominates NOMA with increasing number of users. This is because of minimum weak set interference. The outage probability for $K \geq N$ is less as compared to the conventional SBD-NOMA discussed above. The same trend is shown in the figure.

Fig. 5.3 shows the outage probability of strong users for $K \geq N$. The outage probability of SBD-NOMA in this scenario is less than the conventional UL NOMA with inter-set interference. The same trend is shown in the figure.

In Fig. 5.4, the outage probability of weak users for $K \geq N$ is shown. As weak users have poor channel gains so their outage probability is quite high as compared to the strong users. Fig. 5.4 shows the same trend. The

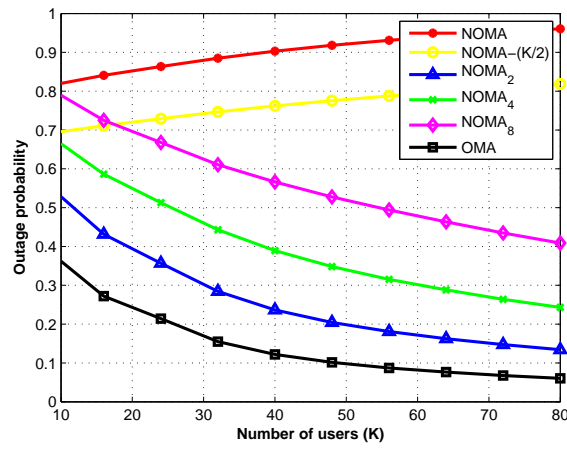


Figure 5.2: Outage probability of SBD-NOMA for $K \geq N$.

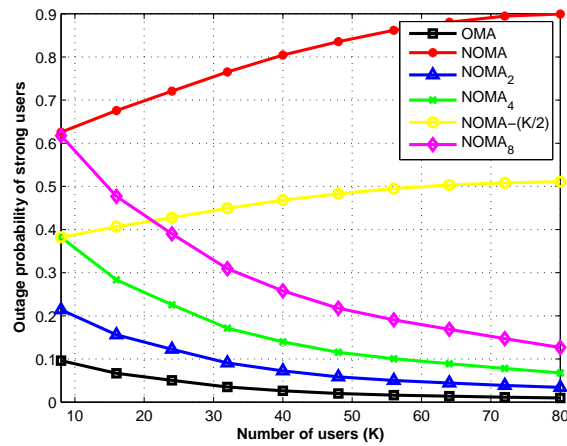


Figure 5.3: Outage probability of strong users for $K \geq N$.

comparison between the analytical and simulations results is shown in Fig.5.5.

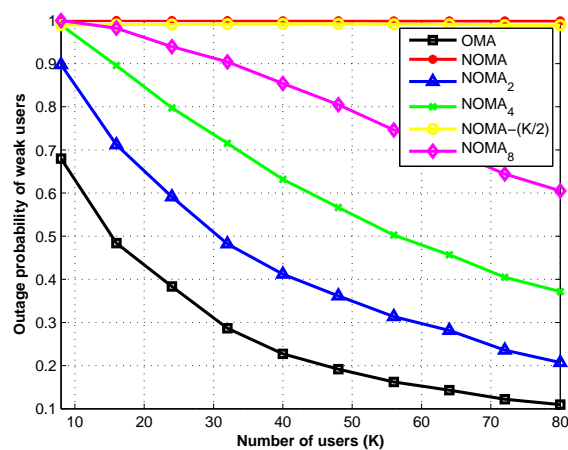


Figure 5.4: Outage probability of weak users for $K \geq N$.

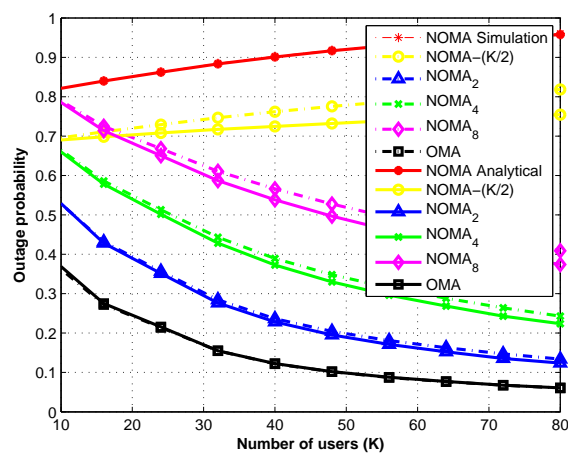


Figure 5.5: Comparison of analytical and simulation result for $K \geq N$.

Chapter 6

Conclusions

This chapter summarize the contributions of this research and also suggest some possible future directions.

In this thesis, we discussed and analyzed the performance of a SBD-NOMA, a promising enabler for 5G. We have investigated the performance of SBD-NOMA, which is an OFDMA-based NOMA system with other multiple access schemes, OMA and NOMA. The paper also discussed the power allocation problem for SBD-NOMA. From a practical implementation point of view, a maximum of 2 users are allowed to share a resource block, however, in this case P users are allowed to share a resource block while the total number of users in the system is K . Approximate closed-form expressions for the outage probability of strong and weak users in SBD-NOMA are derived. The performance gap is evaluated in terms of several metrics and parameters e.g., outage capacity, energy efficiency, sum rate etc. The results presented herein paint a favorable picture that SBD-NOMA performs better than NOMA in terms of achievable rates. The proposed SBD scheme also offered better sum rates with reduced complexity especially in massive access scenarios. The proposed scheme with under different path loss and

power allocation outperformed the EPAS and FPA schemes.

As possible future directions of this research work, we suggest the following:

- Working with imperfect CSI rather than perfect CSI.
- Including massive MIMO technology.
- Working on receiver designing for more optimization.
- Extending this work to multi-cell scenario.
- Incorporating Antenna selection.
- Working with the proposed SBD-NOMA in downlink and changing the scenario accordingly.

Appendix A

Concavity of Sum rate

A.1 Proof of Lemma 1

The achievable sum rate of the system given by (3.16) is expanded as

$$R_{sum} = \frac{1}{\ln 2} \sum_m W_{sb} R_{rr}, \quad (\text{A.1})$$

where

$$\begin{aligned} R_{rr} = & \ln \left(\|\mathbf{z}_{1,n} \cdot \mathbf{h}_{1,n}\|^2 \alpha_{1,n} + \sum_{j=1, j \neq n}^{P/2} \|\mathbf{z}_{1,n} \cdot \mathbf{h}_{1,j}\|^2 \alpha_{1,j} + \sum_{j=1}^{P/2} \|\mathbf{z}_{1,n} \cdot \mathbf{h}_{2,j}\|^2 \alpha_{2,j} + \sigma_n^2 \right) \\ & - \ln \left(\sum_{j=1, j \neq n}^{P/2} \|\mathbf{z}_{1,n} \cdot \mathbf{h}_{1,j}\|^2 \alpha_{1,j} + \sum_{j=1}^{P/2} \|\mathbf{z}_{1,n} \cdot \mathbf{h}_{2,j}\|^2 \alpha_{2,j} + \sigma_n^2 \right) - \ln \left(\sum_{j=1, j \neq n}^{P/2} \|\mathbf{z}_{2,n} \cdot \mathbf{h}_{2,j}\|^2 \alpha_{2,j} + \sigma_n^2 \right) \\ & + \ln \left(\sum_{j=1, j \neq n}^{P/2} \|\mathbf{z}_{2,n} \cdot \mathbf{h}_{2,j}\|^2 \alpha_{2,j} + \sigma_n^2 + \|\mathbf{z}_{2,n} \cdot \mathbf{h}_{2,n}\|^2 \alpha_{2,n} \right), \quad (\text{A.2}) \end{aligned}$$

For notational simplicity, let $\varphi_{an} = \|\mathbf{z}_{1,n} \cdot \mathbf{h}_{1,n}\|^2$, $\varphi_{bn} = \|\mathbf{z}_{2,n} \cdot \mathbf{h}_{2,n}\|^2$, $\varphi_{cn} = \|\mathbf{z}_{1,n} \cdot$

$\mathbf{h}_{2,n}||^2$ and $\varphi_{cjn} = ||\mathbf{z}_{1,n} \cdot \mathbf{h}_{2,j}||^2$.

$$\begin{aligned}
R_{sum} = & \frac{1}{\ln 2} \sum_m W_{sb} \left[\ln \left(\varphi_{an} \alpha_{1,n} + \sum_{j=1, j \neq n}^{P/2} \varphi_{ajn} \alpha_{1,j} + \sum_{j=1}^{P/2} \varphi_{cjn} \alpha_{2,j} + \sigma_n^2 \right) \right. \\
& \quad \left. + \ln \left(\sum_{j=1, j \neq n}^{P/2} \varphi_{bjn} \alpha_{2,j} + \sigma_n^2 + \varphi_{bn} \alpha_{2,n} \right) \right. \\
& \quad \left. - \ln \left(\sum_{j=1, j \neq n}^{P/2} \varphi_{ajn} \alpha_{1,j} + \sum_{j=1}^{P/2} \varphi_{cjn} \alpha_{2,j} + \sigma_n^2 \right) - \ln \left(\sum_{j=1, j \neq n}^{P/2} \varphi_{bjn} \alpha_{2,j} + \sigma_n^2 \right) \right],
\end{aligned} \tag{A.3}$$

To prove Lemma 1, we need to find the Hessian matrix of (A.2). For this, take the second derivative with respect to $\alpha_{1,n}$ and $\alpha_{2,n}$.

$$\partial R_{rr} / \partial \alpha_{1,n}^2 = \frac{-\varphi_{an}^2}{(\varphi_{an} \alpha_{1,n} + \sum_{j=1, j \neq n}^{P/2} \varphi_{ajn} \alpha_{1,j} + \sum_{j=1}^{P/2} \varphi_{cjn} \alpha_{2,j} + \sigma_n^2)^2} \tag{A.4}$$

$$\begin{aligned}
\partial R_{rr} / \partial \alpha_{2,n}^2 = & \frac{-\varphi_{cn}^2}{(\varphi_{an} \alpha_{1,n} + \sum_{j=1, j \neq n}^{P/2} \varphi_{ajn} \alpha_{1,j} + \sum_{j=1}^{P/2} \varphi_{cjn} \alpha_{2,j} + \sigma_n^2)^2} \\
& + \frac{\varphi_{cn}^2}{(\sum_{j=1, j \neq n}^{P/2} \varphi_{ajn} \alpha_{1,j} + \sum_{j=1}^{P/2} \varphi_{cjn} \alpha_{2,j} + \sigma_n^2)^2} \\
& - \frac{\varphi_{bn}^2}{(\sum_{j=1, j \neq n}^{P/2} \varphi_{bjn} \alpha_{2,j} + \sigma_n^2 + \varphi_{bn} \alpha_{2,n})^2}
\end{aligned} \tag{A.5}$$

$$\partial R_{rr} / \partial \alpha_{1,n} \partial \alpha_{2,n} = \frac{-\varphi_{an} \varphi_{cn}}{(\varphi_{an} \alpha_{1,n} + \sum_{j=1, j \neq n}^{P/2} \varphi_{ajn} \alpha_{1,j} + \sum_{j=1}^{P/2} \varphi_{cjn} \alpha_{2,j} + \sigma_n^2)^2} \tag{A.6}$$

As the Hessian matrix is negative semi-definite, because for any vector the answer will always be ≤ 0 , which implies that it is concave in nature. This has been proved by following the arguments similar to the one made in [21].

Bibliography

- [1] I. Chih-Lin, C. Rowell, S. Han, Z. Xu, G. Li, and Z. Pan, “Toward green and soft: A 5G perspective,” *IEEE Commun. Mag.*, vol. 52, no. 2, pp.66–73, 2014.
- [2] J. Thompson, X.-L. Ge, H.-C. Wu, R. Irmer, H. Jiang, G. Fettweis, and S. Alamouti, “5G wireless communication systems: Prospects and challenges,” *IEEE Commun. Mag.*, vol. 52, no. 2, pp.62–64, 2014.
- [3] P. Wang, J. Xiao, and L. Ping, “Comparison of orthogonal and non orthogonal approaches to future wireless cellular systems,” *IEEE Veh. Technol. Mag.*, vol. 1, no. 3, pp.4–11, 2006.
- [4] Y. Saito, Y. Kishiyama, A. Benjebbour, T. Nakamura, A. Li, and K. Higuchi, “Non-orthogonal multiple access (NOMA) for cellular future radio access,” *77th IEEE Veh. Technol. Conf. (VTC Spring)*, 2013.
- [5] Z. Ding, F. Adachi, and H. V. Poor, “The application of MIMO to non-orthogonal multiple access,” *IEEE Trans. Wireless Commun.*, vol. 15, no. 1, pp.537-552, 2016.
- [6] Z. Ding, Z. Yang, P. Fan, and H. V. Poor, “On the performance of non-orthogonal multiple access in 5G systems with randomly deployed users,” *IEEE Signal Process. Lett.*, vol. 21, no. 12, pp.1501–1505, 2014.

- [7] K.Higuchi, Y.Kishiyama, "Non-orthogonal access with random beamforming and intra-beam SIC for cellular MIMO downlink," *IEEE 78th Veh. Technol. Conf. (VTC Fall)*, 2013.
- [8] S.Qi, S.Han, I.Chin-Lin, and Z.Pan, "On the ergodic capacity of MIMO NOMA systems," *IEEE Wireless Commun. Lett.*, vol. 4, no. 4, pp.405-408, 2015.
- [9] B. Kim, W.Chung, S.Lim, S.Suh, J.Kwun, S.Choi, and D.Hong, "Uplink NOMA with multi-antenna," *81st IEEE Veh. Technol. Conf. (VTC Spring)*, pp.1-5, 2015.
- [10] Z.Ding, P.Fan, and V.Poor, "Impact of user pairing on 5G non-orthogonal multiple access downlink transmissions." *IEEE Trans. Veh. Technol*, vol. 65, no. 8, pp. 6010-6023, 2016.
- [11] M.Al-Imari, P.Xiao, M.A.Imran, and R.Tafazolli, "Uplink non-orthogonal multiple access for 5G wireless networks," *11th International Symposium on Wireless Communications Systems (ISWCS)*, pp.781-785, 2014.
- [12] S. Qureshi, S. A. Hassan, "MIMO uplink NOMA with successive bandwidth division," *IEEE Wireless Commun. Networking. Conf. (WCNC Workshops)*, pp.481-486, 2016.
- [13] S.Chen, K.Peng, and H.Jin, "A suboptimal scheme for uplink NOMA in 5G systems," *IEEE International Wireless Commun. and Mobile Computing Conf. (IWCMC)*, pp.1429-1434, 2015.
- [14] S. A. R. Naqvi, S. A. Hassan "Combining NOMA and mmWave technology for cellular communication," *IEEE Veh. Technol. Conf. (VTC Fall)*, Sep 2016.

- [15] Z.Ding, M.Peng, and H.V.Poor, “Cooperative non-orthogonal multiple access in 5G systems,” *IEEE Commun. Lett.*, vol. 19, no. 8, pp.1462–1465, 2015.
- [16] M. R. Hojeij, J. Farah, C. Nour, and C. Douillar, “Resource allocation in downlink non-orthogonal multiple access (NOMA) for future radio access,” *81st IEEE Veh. Technol. Conf. (VTC Spring)*, pp.1–6, 2015.
- [17] Y. Saito, A. Benjebbour, Y. Kishiyama, and T. Nakamura, “System-level performance evaluation of downlink non-orthogonal multiple access (NOMA),” *PIMRC*, pp.611–615, 2013.
- [18] Z. Q. Al-Abbasi and D. K. C. So, “Power allocation for sum rate maximization in non-orthogonal multiple access system,” *IEEE 26th Annual International Symposium on Personal, Indoor, and Mobile Radio Communications (PIMRC)*, pp.1649–1653, 2015.
- [19] P. Parida and S. S. Das, “Power allocation in OFDM based NOMA systems: A DC programming approach,” *IEEE Global Telecommun. Conf. (GLOBECOM Workshops)*, 2014.
- [20] N. Otao, Y. Kishiyama, and K. Higuchi, “Performance of non-orthogonal multiple access with SIC in cellular downlink using proportional fair-based resource allocation,” *IEICE Trans Commun.*, vol. 98, no. 2, pp.344–351, 2015.
- [21] J.Choi, “On the power allocation for MIMO-NOMA systems with layered transmissions,” *IEEE Trans. Wireless Commun.*, vol. 15, no. 5, pp.3226–3237, 2016.

- [22] Li GY, He C, Zheng F-C, You X, “Energy-efficient resource allocation in OFDM systems with distributed antennas,” *IEEE Trans Veh. Technol.*, vol. 63, no. 3, pp.1223–1231, 2014.
- [23] Z.Shen, J.G. Andrews, and B.L. Evans, “Adaptive resource allocation in multiuser OFDM systems with proportional rate constraints,” *IEEE Trans. Wireless Commun.*, vol. 4, no. 6, pp.2726–2737, 2005.
- [24] S. Qureshi, S. A. Hassan, and D. Nalin K. Jayakody, “Successive Bandwidth Division NOMA Systems: Uplink Power Allocation with Proportional Fairness,” *IEEE Consumer Commun. and Networking Conf. (CCNC)*, 2017.
- [25] M. S. Zia and S. A. Hassan, “On the Impacts of Composite Fading on Large-Scale Multi-user MIMO Systems,” *IEEE Commun. Lett.*, vol. 19, no. 12, pp. 2286-2289, 2015.
- [26] S. A. Hassan and M. Ann Ingram, “The Benefit of co-locating groups of nodes in cooperative line networks,” *IEEE Commun. Lett.*, vol. 16, no. 2, pp. 234-237, 2012.
- [27] M. S. Zia and S. A. Hassan, “Outage Analysis of Multi-User Massive MIMO Systems Subject to Composite Fading“, *81st IEEE Veh. Technol. Conf. (VTC Spring)*, 2015.
- [28] M. Bacha and S. A. Hassan, “Coverage Aspects of Cooperative Multi-hop Line Networks in Composite Fading Environment“, *IEEE Intl. Wireless Commun. and Mobile Computing Conf. (IWCMC)*, 2014.
- [29] A. Afzal and S. A. Hassan, “A Stochastic Geometry Approach for Outage Analysis of Ad Hoc SISO Networks in Rayleigh Fading,” *IEEE Global Commun. Conf. (Globecom)*, 2013.

- [30] S. A. Hassan and P. Wang, "Dual relay communication system: Channel capacity and power allocations," *10th IEEE Intl. Wireless and Microwave Technol. Conf. (WAMICON)*, 2009.
- [31] Z. Ding, R. Schober and H. V. Poor, "A general MIMO framework for NOMA downlink and uplink transmission based on signal alignment," *in CoRR abs/1508.07433*, 2015.
- [32] S. A. Hassan and M. Ann Ingram, "A quasi-stationary Markov Chain model of a cooperative multi-hop linear network," *IEEE Trans. Wireless Commun.*, vol. 10, no. 7, pp. 2306-2315, 2011.
- [33] P. Li, D. Paul, R. Narasimhan and J. Cioffi, "On the distribution of SINR for the MMSE MIMO receiver and performance analysis," *IEEE Trans. Inf. Theory*, vol. 52, no. 1, pp. 271-286, 2006.
- [34] B. Sklar, "Rayleigh fading channels in mobile digital communications systems part I: Characterization," *IEEE Commun. Mag.*, vol. 35, no. 7, pp. 90100, Jul. 1997.
- [35] Y. Jiang, M. Varanasi, and J. Li, "Performance analysis of ZF and MMSE equalizers for MIMO systems: An in-depth study of the high SNR regime," *IEEE Trans. Inf. Theory*, vol. 57, no. 4, pp. 2008-2026, Apr. 2011.
- [36] H. Li and A. G. Armada, "Bit error rate performance of MIMO MMSE receivers in correlated Rayleigh at-fading channels," *IEEE Trans. Veh. Technol.*, vol. 60, no. 1, pp. 313-317, Jan. 2011.
- [37] N. Kim, Y. Lee and H. Park, "Performance analysis of MIMO system with linear MMSE receiver", *IEEE Trans. Wireless Commun.*, vol. 7, no.11, pp. 4474-4478, 2008.

- [38] H. Q. Ngo, M. Matthaiou, T. Q. Duong, E. G. Larsson, “Uplink performance analysis of multicell MU-SIMO systems with ZF receivers,” *IEEE Trans. Veh. Technol.*, vol. 62, no. 9, pp. 4471-4483, Nov. 2013.
- [39] A. F. Molisch, *Wireless Communication*. Wiley-IEEE Press, 2005.
- [40] R. Hu and Y. Qian, “An energy efficient and spectrum efficient wireless heterogeneous network framework for 5G systems”, *IEEE Commun. Mag.*, vol. 52, no. 5, pp. 94-101, 2014.
- [41] H. Pervaiz, L. Musavian, and Q. Ni, “Energy and spectrum efficiency trade-off for Green Small Cell Networks,” *IEEE International Conf. on Commun. (ICC)*, pp. 5410-5415, 2015.